Available online at www.sciencedirect.com
SCIENCE DIRECT®
Optics Communications 242 (2004) 115–122
OPTICS COMMUNICATIONS
www.elsevier.com/locate/optcom

Photo-induced birefringence and polarization holography in polymer films containing spirooxazine compounds pre-irradiated by UV light

Shencheng Fu [a], Yichun Liu [a,*], Zifeng Lu [a], Lin Dong [b], Weilin Hu [c], Minggui Xie [c]

[a] *Center for Advanced Optoelectronic Functional Material Research, Northeast Normal University, 5268 Renmin Street, Changchun 130024, PR China*

[b] *Key Laboratory of Excited State Processes, Changchun Institute of Optics, Fine Mechanics and Physics, Chinese Academy of Sciences, 16-Dongnanhu Avenue, Changchun 130021, PR China*

[c] *Faculty of Chemistry, Sichuan University, Chengdu 610064, PR China*

Received 16 June 2004; received in revised form 26 July 2004; accepted 10 August 2004

Abstract

Photo-induced birefringence of spirooxazine (6′-piperidino-1,3,3-trimethylspiro[indolino-2,3′-[3H]naphtha-[2,1-b][1,4]oxazine] in poly(methyl methacrylate) films pre-irradiated by ultraviolet light was investigated as a function of He–Ne laser (632.8 nm) pumping-beam intensity. A phenomenological model, taking photo-orientation and photo-isomerization into account, is in good agreement with the measurements. This material exhibited a competing process between photo-orientation and photo-isomerization. The photo-orientation is predominant when the power density of He–Ne beam is lower; while the photo-isomerization is dominant at relatively high power density of He–Ne beam. In terms of these effects, a comparison between (s,s) and (s,p) holographic gratings optically recorded by He–Ne laser of 632.8 nm in this composite film pre-irradiated by UV light was also investigated.

PACS: 78.20.Fm; 42.70.Ln; 42.40.Eq
Keywords: Photo-induced birefringence; Polarization holography; Spirooxazine; He–Ne laser; UV-light irradiation

1. Introduction

Spirooxazines (SOs) and spiropyrans (SPs) are typical organic compounds exhibiting photochro-

* Corresponding author. Tel.: +86 431 5099168; fax: +86 431 5684009.
E-mail address: ycliu@nenu.edu.cn (Y. Liu).

0030-4018/$ - see front matter © 2004 Elsevier B.V. All rights reserved.
doi:10.1016/j.optcom.2004.08.022

mism. Recently, photochromism of SOs has been the subject of considerable research interest [1–7]. Compared to SPs, SOs show better fatigue resistance and photostability [8,9], which provides a possibility of practical applications in lenses of variable optical density, displays, filters and optical-memory devices. Photochromic feature of SOs and SPs arises from carbon–oxygen (C_{spiro}–O) bond cleavage of the colorless spiro form upon UV-light excitation and subsequent isomerization to colored open forms which are called photomerocyanines (PMCs). PMCs can revert to the initial spiro forms thermally or photochemically. SOs are transparent with low non-linear optical properties, while PMCs are blue and highly non-linear because of their non-centre symmetry and electron conjugation ($\beta\mu < 0$) [10]. Just like azo molecules, PMC molecules will continue to absorb the polarized writing beam as long as a component of their electric dipole moment lies in the direction of polarization of the beam. After several PMC–SO–PMC recycles accompanied by UV irradiation, an accumulation of molecules aligned perpendicularly to the pumping beam polarization direction occurs [11]. The macroscopic equilibrium state becomes anisotropic, resulting in photo-induced birefringence. Studying the dynamics of the photo–induced birefringence can give information about the orientation dynamics of the dye molecules in the poly(methyl methacrylate) (PMMA) matrix, which is of fundamental importance for device development [12]. Photo-induced birefringence is used successfully in polarization holography, because it allows recording of the interference of two waves with orthogonal polarizations. Polarization holography [13] provides many significant advantages such as the possibility of selecting only the diffracted beam and the capability of recording holographic information of different objects on a specific area of the recording media simply by changing the direction of polarization of the recording beams [14], i.e., high-density optical storage. Previously, most studies of optical information storage in spirooxazines focused on UV, Ar^+ and CO_2 laser holographic recording [15–17]. However, little attention has been given to photo-induced birefringence and polarization holographic recording for spirooxazines with red light, which will be of great importance for practical applications.

This paper describes in detail the results of investigation of photo-induced birefringence with pumping light of 632.8 and holographic recordings (s, s and s, p) at 632.8 for 6′-piperidino-1,3,3-trimethylspiro[indolino-2,3′-[3H]naphtha-[2,1-b][1,4]-oxazine doped PMMA films pre-irradiated by UV light.

2. Experiment

2.1. Materials and film preparation

The chemical structures of 6′-piperidino-1,3,3-trimethylspiro[indolino-2,3′-[3H]naphtha-[2,1-b][1,4]oxazine (SO-1) and the corresponding UV-induced photomerocyanine (PMC) are shown in Fig. 1. SO-1 was synthesized with microwave irradiation [18]. Commercially available PMMA was used without further purification. Both SO-1 and PMMA were dissolved in $CHCl_3$ and then cast on a clean glass substrate. After the solvent evaporated, the composite film was obtained and used for measurements of photo-induced birefringence and for polarization holographic recording. The pre-set dye concentration was 5.0 wt% and typical film thickness was 10±1 μm measured with a Precision Ellipsometer.

2.2. UV–Vis spectra

The UV–Vis spectra were measured using a Perkin–Elmer Lambda 900 spectrophotometer with a range of 190–3200 nm. Typical UV–Vis spectra of PMMA film containing SO-1 and the corresponding UV-induced PMC are shown in Fig. 2, as dashed lines and dotted lines, respectively. Thermal relaxation of PMC in darkness (25 °C) is also shown (solid lines). The inset is the absorption coefficient at 633 nm as a function of the time the UV light is switched off. After about 4 hours the film still contains many PMC molecules. The decoloration dynamic at 633 nm was fitted by the following equation:

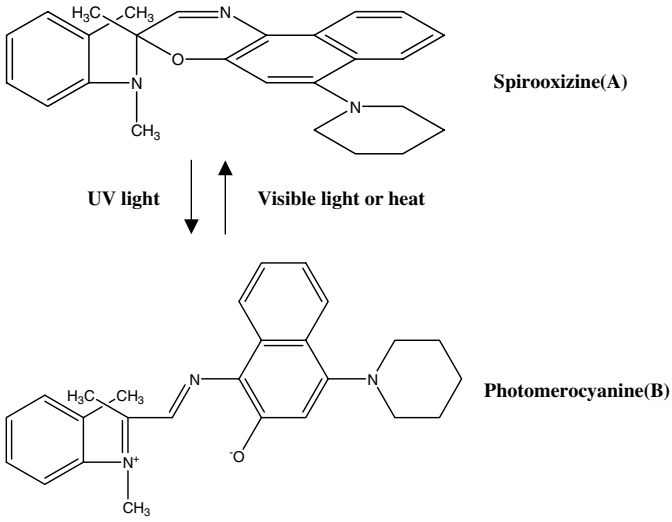

Fig. 1. Chemical structure of SO-1 and corresponding UV-induced PMC form.

$$\ln\left(\frac{A_t - A_\infty}{A_0 - A_\infty}\right) = -\frac{t}{\tau},$$

where A_t, A_0 and A_∞ are the absorbencies at $\lambda = 633$ nm at times t, zero and infinity, respectively. A value of $\tau = 45$ min is obtained. The characteristic spectral bands at 365 nm correspond to the π–π* electronic transition for both SO-1 and PMC, while the absorption near 633 nm corresponds to the n–π* electronic transition and intermolecular charge-transfer of PMC [19].

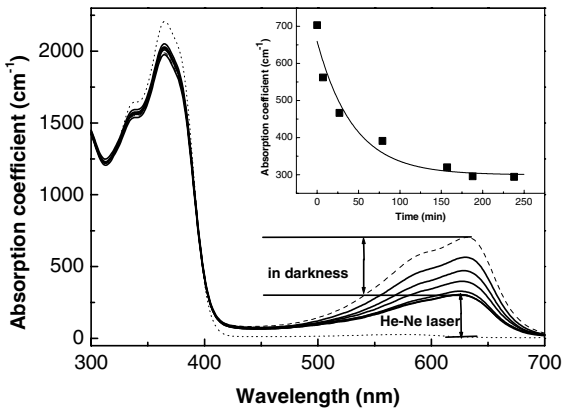

Fig. 2. UV–Vis spectrum of PMMA film doped with 5 wt% SO-1 (dotted line), the corresponding spectrum after UV-induced isomerization of SO-1 to PMC (dashed line) and changes in the absorbance spectra of PMC in darkness (solid lines). The inset is the absorption coefficient at 633 nm according to the time the UV light is switched off. The square dots are the experimental measurements. The solid line is the theoretical fit.

2.3. Optical setup

For the photo-induced birefringence measurements, two laser beams were nearly parallel incident to the sample, as shown in Fig. 3(a). The major elements of the experimental apparatus were a linearly polarized He–Ne laser (632.8 nm) pumping beam and a linearly polarized double-frequency Nd:YAG laser (532 nm) probe beam. A mercury arc lamp (125 mW) provided homogenous, incoherent light at 365 nm, to irradiate the sample. And the power density of the mercury arc lamp at the sample location is about 1 mW/cm^2. A half-wave plate allowed rotation of the pumping-beam polarization axis. Samples were placed between two crossed polarizers in the path of the probe beam, at the point of intersection with the pumping beam. The diameters of the two laser beams are both about 0.3 cm. Probe beam transmittance was registered on a CCD (sensitive region from 350 to 900 nm) and the resulting signal was acquired by a computer. Fig. 3(b) shows the optical configuration for holographic recording with

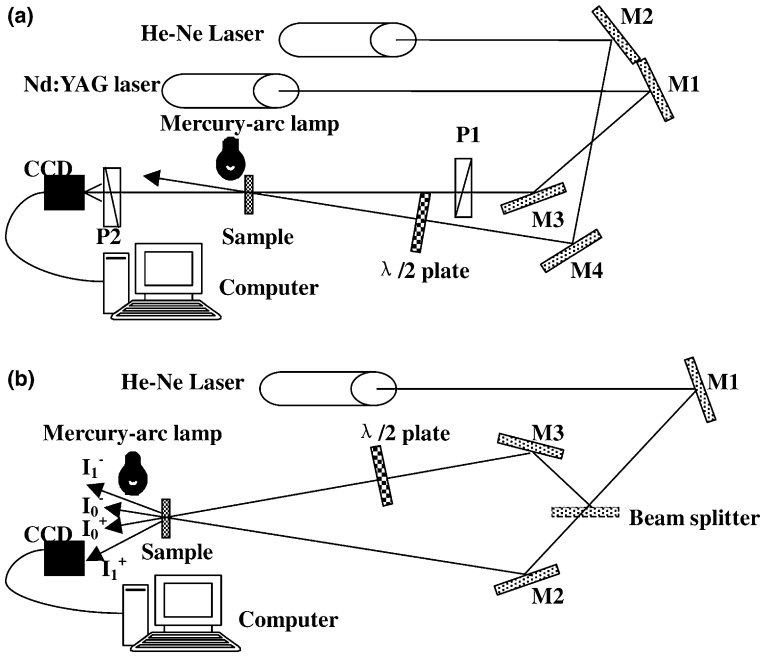

Fig. 3. (a) Experimental configuration for photo-induced birefringence accompanied by UV-light irradiation. (b) Experimental configuration for the recording of holographic gratings by two He–Ne beams with parallel or orthogonal polarization.

two parallel or orthogonal polarized beams. The intersecting angle between the two beams was set at approximately 10°.

3. Results and discussion

3.1. Polarized-light induced birefringence in UV-irradiated films

PMMA films containing photochromic SO-1 were exposed to UV irradiation at 365 nm and pumping at 632.8 nm. Probe-beam transmittance result is shown in Fig. 4. Because PMC absorbs at 532 nm, the probe-beam power was held at 0.1 mW, incident on the sample with a beam area of 0.07 cm^2. The polarization angle between the pumping and probe beams was 45°.

The film was exposed to UV irradiation until maximal coloration was observed, at which point no transmittance signal was detected, indicating random PMC orientation in the film. Then, at time zero in Fig. 4, with the UV source still on, the pumping beam was turned on (10 mW He–Ne power) and the measured transmittance increased rapidly to a maximum value, then decreased grad-

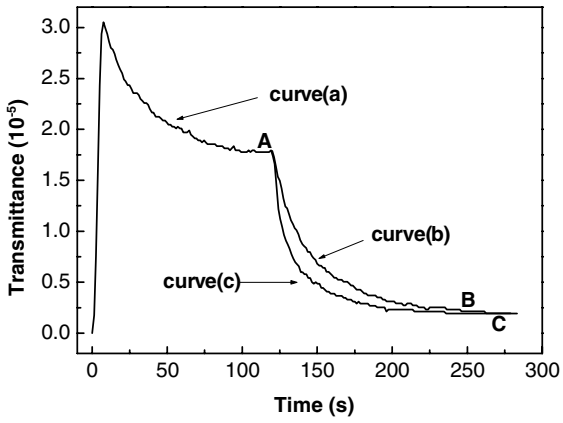

Fig. 4. The transmittance of 532 nm (double-frequency of Nd:YAG laser) versus exposure time with the pumping light (632.8 nm) of 10 mW and the polarization angles between 532 nm laser beam and the He–Ne beam of 45°. Curve a: UV light and He–Ne beams are both on until point A. Curve b: He–Ne laser beam is switched off. Curve c: UV light is switched off.

ually to a fixed value (point A) (curve a). When the pumping beam was turned off, while the UV source remained on, the transmittance decreased further and approached a constant value at point B (curve b). Alternatively, when the UV source was turned off at point A, and the pumping beam remained on, the measured transmittance decreased gradually to point C (curve c).

These experimental observations can be explained as follows:

$$\text{SO-1(isotropic)} \underset{\text{He–Ne beam}}{\overset{\text{UV light}}{\rightleftarrows}} \text{PMC(isotropic)}$$

$$\underset{\text{thermally}}{\overset{\text{He–Ne beam}}{\rightleftarrows}} \text{PMC(antisotropic)}$$

PMC has an extremely large dipole moment because of its ionic form, while the dipole moment of SO-1 is relatively small [10,20,21]. Hence, the birefringence induced by the orientation of SO-1 is neglected. And the dark time (45 min) is so long that thermal relaxation from PMC to SO-1 is ignored. The nearly instantaneous increase to maximum transmittance is attributed to the rapid reorientation of PMC induced by the linearly polarized He–Ne pumping beam. At the same time, the He–Ne laser also drives conversion of PMC to SO-1. However, the UV light drives the competing reverse reaction of SO-1 to PMC. The PMC molecules will continue to absorb the He–Ne pumping beam as long as a component of its electric dipole moment lies in the direction of the polarization of the beam competing with the thermal randomization. Eventually, chemical species equilibrium between SO-1 and PMC and reorientation equilibrium for PMC molecules are reached at point A in Fig. 4. When He–Ne laser is turned off at point A, incoherent UV light drives the remaining SO-1 molecules to PMC with random orientation. Also, the PMC molecules initially oriented by the linearly polarized He–Ne beam are randomized thermally. Consequently, the transmittance decreases gradually to point B. The transmittance at point B is not to zero, which is attributed to residual PMC molecules that are trapped by the PMMA matrix and keep their orientation. When the UV light is switched off at point C with the He–Ne laser still on, most of the PMC molecules are transformed to SO-1 by the pump radiation and also randomized thermally, so a similar result is observed.

To investigate the dependence of photo-induced birefringence on He–Ne laser intensity, the power density of He–Ne laser was varied from 0/0.07 to 35/0.07 mW/cm^2. The mercury arc lamp was held constant at 125 mW. Fig. 5 shows the measured values of equilibrium birefringence as a function of the He–Ne power density (square dots). With increasing He–Ne power density, equilibrium birefringence rises at first and then drops gradually. These observations can be explained as the result of a competing process between photo-orientation and photo-isomerization induced by He–Ne laser.

There are two main factors affecting the variation of the equilibrium birefringence. One is the efficiency of He–Ne pumping beam, and the other is the total number of PMC molecules at the equilibrium state. When the total number of PMC molecules at the equilibrium state is considered constant, Blanche's ''two-layer model'' [22] is suitable for experiment. The photo-induced birefringence (Δn) increases with the intensity of the pumping beam in the region of relatively low He–Ne intensity. The higher the He–Ne laser

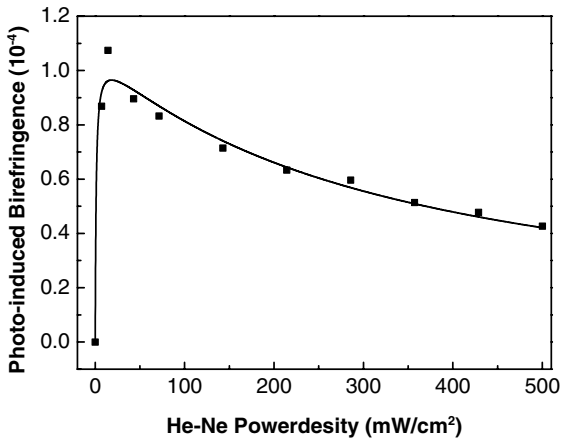

Fig. 5. The equilibrium transmittance of 532 nm laser versus the He–Ne power density with the polarization angles between 532 nm laser beam and the He–Ne beam of 45°. The square dots are the experimental values. The solid line is the theoretical fit.

intensity, the higher the number of PMC molecules that are aligned with the beam polarization. The behavior of Δn can be described by the following phenomenological equation [22],

$$\Delta n = \frac{aeIB}{1+eI},$$

where a is the maximum photo-induced birefringence, e is the efficiency with which the light induces birefringence, I is the intensity of the He–Ne beam and B is the concentration of the PMC molecules, which is in proportion to the total number of PMC molecules. However, Δn tends to be constant at relatively high pumping intensity because there is a saturation when all molecules are aligned. At this time, it should be taken into account that the total number of PMC molecules at the equilibrium state is changed by He–Ne laser.

$$\mathrm{A(SO\text{-}1)} \underset{R_{\mathrm{B}}(\lambda_b),R_T}{\overset{R_{\mathrm{A}}(\lambda_{\mathrm{A}})}{\leftrightarrows}} \mathrm{B(PMC)}$$

$$-\frac{\mathrm{d}B}{\mathrm{d}t} = R_{\mathrm{B}}B - R_{\mathrm{A}}A + R_T B = R_{\mathrm{B}}B - R_{\mathrm{A}}A_0 + R_{\mathrm{A}}B + R_T B,$$

where A is the concentration of the SO-1 molecules, R_{A} and R_{B} are the photochemical rate constants for the colorless (SO-1) and colored (PMC) forms, and R_T is the rate constant for thermal conversion of B to A. R_i is proportional to the light intensity (J cm^{-2} s^{-1}) at wavelength λ_i, A_0 is the total concentration of all the dye species, satisfying

$$A_0 = A(t) + B(t).$$

When the photo-equilibrium is reached,

$$\frac{\mathrm{d}B}{\mathrm{d}t} = 0.$$

And the concentration of the PMC molecules is determined by:

$$B = \frac{R_{\mathrm{A}}A_0}{R_{\mathrm{A}} + R_{\mathrm{B}} + R_T} = \frac{c}{I+b}.$$

b and c are simplified constant as R_{A}, A_0 and R_T are constant in this experiment. The higher the He–Ne intensity, the fewer the total number of PMC molecules at the equilibrium state. That is, the photo-isomerization from PMC to SO-1 is predominant when the power density of He–Ne beam is higher; while the photo-orientation is dominant at relatively low power density of He–Ne beam. Hence, when the two main factors are both taken into account, the behavior of Δn can be described as the following equation,

$$\Delta n = \frac{aeI}{1+eI} \cdot \frac{c}{I+b}.$$

The result of such a fit is also presented in Fig. 5 (solid line). The model is in relatively good agreement with the measurements.

3.2. Polarization holographic recording accompanied by UV-light irradiation

Kakichashvili and Shaverdova [23] reported that materials which present photo-anisotropy (Weignert effect [24]) could be used in the recording of the interference of two coherent non-parallel polarized overlapping beams. They termed this recording as polarization holography. In this case, the resulting light field is not modulated in intensity, but a similar pattern of information is created by means of the polarization states which are modulated consequently to the optical path difference [25].

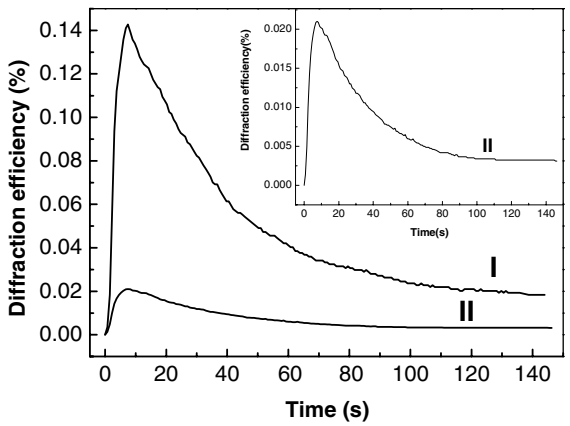

Fig. 6. The first-order diffractive signal of the holographic gratings pre-irradiated by UV-light versus time with the same (**I**) or different (**II**) polarized recording beams. The inset is the magnification of curve (**II**).

Fig. 6 shows the first-order diffractive signal of the holographic gratings recorded by two He–Ne beams in the same(s,s) (**I**) or different (s,p) (**II**) polarization. The inset of Fig. 6 is the magnification of curve (**II**). The sample was initially exposed to the UV excitation beam, until maximal coloring occurred, then separately exposed to two parallel or orthogonal polarized He–Ne beams (632.8 nm) of 10 mW. Each beam acts as both writing beam and reading beams. The Nd:YAG laser is not used to read the holographic gratings in order to reduce unnecessary loss of diffraction efficiency. The first-order diffractive signal of the holographic gratings was received by CCD. On turning on the He–Ne laser, the diffractive signal rapidly reaches a maximum value, and then drops slowly to a steady value. Scalar (s,s) gratings are formed by both the isomerization from PMC to SO-1 and the orientation of PMC molecules, which result in the formations of isomerization and orientation gratings, respectively. A competing process occurs between the isomerization gratings and the orientation gratings after UV pre-irradiation. The diffraction efficiency rapidly reaches the maximum value when the two competitive gratings create the optimal proportion. Continuing the illumination of He–Ne laser, the orientation gratings are weakened with a decrease of the number of PMC molecules. Eventually, the isomerization gratings predominate in the film and the value of diffraction efficiency tends to be steady value. For (s,p) gratings, the diffractive signal is only created by formation of orientation grating for PMC and erased by thermal randomization and decreasing population of PMC, which is transformed to SO-1 by the He–Ne beam. So the diffraction efficiency of (s,p) gratings is lower than that of (s,s) gratings. The diffraction efficiency of (s,p) gratings drops almost to zero at time 140 s. However, the polarization holographic gratings contain multi-information, such as phase, amplitude and polarization, which will promote the density of optical storage. The result indicates that it is possible to perform polarization holography at 632.8 nm accompanied by UV pre-irradiation with this material.We are trying presently to mix SO-1 into another matrix to overcome the drawback of the decrease of photo-induced birefringence or diffraction efficiency after initial increase. A more-detailed investigation seems to be promising.

4. Conclusion

Photo-induced birefringence of PMMA films containing 6′-piperidino-1,3,3-trimethylspiro [indolino-2,3′-[3H]naphtha-[2,1-b][1,4]oxazine pre-irradiated by UV light was related to the intensity of the pumping light. A phenomenological model, taking photo-isomerization and photo-orientation into account, is in good agreement with the measurements. The competition between the photo-orientation and the photo-isomerization induced by He–Ne laser was exhibited after UV pre-irradiation. Polarization holographic gratings were recorded by He–Ne laser light at 632.8 nm accompanied by UV pre-irradiation in PMMA films containing spirooxazines.

Acknowledgements

This work was supported by the National Natural Science Foundation of China (60176003), the Foundational Excellent Researcher to Go beyond Century of Ministry of Education of China, and Science Foundation for Young Teachers of Northeast Normal University.

References

[1] G. Berkovic, V. Krongauz, V. Weiss, Chem. Rev. 100 (2000) 1741.
[2] Roni A. Kopelman, Sean M. Snyder, Natia L. Frank, J. Am. Chem. Soc. 125 (2003) 13684.
[3] V.M. Anisimov, S.M. Aldoshin, Theoret. Chem. 419 (1997) 77.
[4] K. Sasaki, T. Nagamura, Appl. Phys. Lett. 71 (1997) 4.
[5] L. Hou, H. Schmidt, Mater. Lett. 27 (1996) 215.
[6] V.S. Marevtsev, N.L. Zaichenko, J. Photochem. Photobiol. A 104 (1997) 197.
[7] A.K. Chibisov, H. Gorner, J. Phys. Chem. 103 (1999) 5211.
[8] N.Y.C. Chu, Can. J. Chem. 61 (1983) 300.
[9] U.W. Grummt, M. Reichenbacher, R. Paetzold, Tetrahedron Lett. 22 (1981) 3945.

[10] S. Hosotte, M. Dumont, Synth. Mater. 81 (1996) 125.
[11] H. Ishitobi, Z. Sekkat, S. Kawata, Chem. Phys. Lett. 300 (1999) 421.
[12] H. Ono, N. Kowatain, N. Kawatsuki, Opt. Mater. 10 (2000) 175.
[13] Sh.D. Kakichashvili, Polarization Holography, Nauka, 1989 (in Russian).
[14] T. Todorov, L. Nikolava, K. Stoyanova, N. Tomova, Appl. Opt. 24 (1985) 785.
[15] V. Weiss, V.A. Krongauz, J. Phys. Chem. 98 (1994) 7562.
[16] V. Weiss, A.A. Friesem, V.A. Krongauz, Opt. Lett. 18 (1993) 1089.
[17] T. Izawa, M. Kamiyama, Appl. Phys. Lett. 71 (1969) 4.
[18] W. Hu, Q. Jiang, K. Zou, Y. Huang, M. Xie, Chem. Res. Appl. 15 (2003) 282.
[19] G.H. Brown, Photochromism, Wiley, New York, 1971.
[20] D.J. Williams, Angew. Chem. Int. Ed. Engl. 23 (1984) 690.
[21] Dulcic, C. Flytzanis, Opt. Commun. 25 (1978) 402.
[22] P.-A. Blanche, Ph.C. Lemaire, C. Maertens, P. Dubois, R. Jérôme, Opt. Commun. 139 (1997) 92.
[23] Sh.D. Kakichashvili, V.D. Shaverdova, Opt. Spectrosc. 41 (1976) 525.
[24] F. Weigert, Ann. Phys. 63 (1920) 682.
[25] T. Todorov, L. Nikolava, N. Tomova, Appl. Opt. 23 (1984) 4309.